Transportation Research Part C 118 (2020) 102685

Contents lists available at ScienceDirect

Transportation Research Part C

journal homepage: www.elsevier.com/locate/trc

Hierarchical density-based clustering methods for tolling zone definition and their impact on distance-based toll optimization

Antonis F. Lentzakis[a,*], Ravi Seshadri[a], Arun Akkinepally[b], Vinh-An Vu[c], Moshe Ben-Akiva[b]

[a] Singapore-MIT Alliance for Research and Technology, 1 CREATE Way, 09-02 CREATE Tower, Singapore 138602, Singapore
[b] Intelligent Transportation Systems Lab, MIT, 77 Massachusetts Avenue, Room 1-181, Cambridge, MA 02139, USA
[c] Relativ, 3-12-2 Motoazabu, Minato-ku, Tokyo 106-0046, Japan

ARTICLE INFO

Keywords:
Distance-based road pricing
Dynamic toll optimization
Density-based clustering

ABSTRACT

Real-time network control strategies such as congestion pricing have been used in a number of metropolitan areas around the world for traffic congestion mitigation. Recent advances in Global Navigation Satellite System (GNSS) technology have led to increasing interest in distance- or usage-based road pricing as an effective alternative to traditional facility-, cordon- and area-based pricing that typically rely on fixed infrastructure. In this paper, we propose the use of feature-variant clustering methods, OPTICS and HDBSCAN*, as a systematic approach for tolling zone definition to operationalize distance-based tolling schemes. Subsequently, we develop a framework for predictive distance-based toll optimization to evaluate network performance for the various tolling zone definitions derived from the aforementioned feature-variant clustering methods. In this framework, for a specific tolling zone definition, tolling function parameters are optimized using a simulation-based Dynamic Traffic Assignment (DTA) model operating within a rolling horizon scheme. Predictive optimization is integrated with the guidance information generation. Behavioral models capture drivers' responses to the tolls in terms of trip cancellation and choices of mode, route and departure time. Experiments on the real-world Expressway and Major Arterials network of Singapore demonstrate improved effectiveness of distance-based toll optimization given tolling zone definitions derived from feature-variant clustering, compared to fixed cordon-based pricing, adaptive cordon-based pricing, as well as distance-based pricing with ad hoc tolling zone definitions. Further, the results indicate that the use of the marginal link cost tolls as a clustering feature produces the most robust tolling zone definitions and yields significant improvements in social welfare over ad hoc zone definitions and cordon-pricing. Finally, experiments on the Boston CBD network also demonstrate the effectiveness of distance-based toll optimization schemes on urban traffic networks.

1. Introduction

Traffic congestion is a pervasive problem world-wide, resulting in significant costs to the commuter, economy and environment. According to the Victoria Transport Policy Institute's Urban Mobility Report (UMR) (Litman, 2014), congestion was estimated to incur 5.5 billion hours of time delay and 2.9 billion gallons of fuel in urban areas of the United States between 2000 and 2010. The

* Corresponding author.
E-mail address: antonios@smart.mit.edu (A.F. Lentzakis).

https://doi.org/10.1016/j.trc.2020.102685
Received 22 December 2019; Received in revised form 18 May 2020; Accepted 31 May 2020

UMR predicted that congestion costs will increase from $121 billion (in 2011) to $199 billion (in 2020).

Congestion pricing is an important approach for traffic management that encourages travelers to adjust their behavior along various dimensions including trip making, destination choice, mode choice, and time of day and route choices (refer de Palma and Lindsey (2011) for a detailed review). Facility-based and cordon/area-based pricing typically depend on physical infrastructure such as gates or gantries to detect when drivers enter or leave the tolled area. Unfortunately, if there is a need to effect changes in the charging facilities/areas or zones, physical gantries are not so easily relocated. Moreover, toll charges are not differentiated based on distance travelled within the tolling zone leading to inefficiency in terms of congestion management.

The aforementioned disadvantages of facility-/area-based pricing and the advancement of Global Navigation Satellite System (GNSS) technology have generated interest in usage-based tolling schemes wherein charges vary in terms of distance-traveled, time spent on traveling or time spent in congestion. An example of the use of GNSS technology in this context is the satellite-based next generation Electronic Road Pricing system in Singapore or ERP 2.0, set to be rolled out in 2020, which provides the ability to charge tolls based on distance traveled or time spent on the network. According to Smith et al. (1994), time-spent-in-congestion-based pricing outperforms distance and time-based pricing because it achieves the greatest increase in network speeds. There is concern, however, that tolls based on time spent traveling and time spent in congestion would be unpredictable, and evidence shows that they potentially encourage unsafe driving (Bonsall and Palmer, 1997). Distance-based pricing circumvents this concern while still addressing issues present in facility-/area-based pricing, such as inflexibility regarding gantry relocation and inefficient toll charging. This has led to distance-based pricing becoming an area of increasing interest in both theory and practice. The approaches in the existing literature differ with regard to the form of the tolling function considered (which translates distance traversed to a toll charge) and model formulation (optimization problem and objective function, demand and supply models), and these are briefly discussed next.

In a distance-based tolling scheme, the network is typically partitioned into a set of zones, and the toll charged is either a linear or a non-linear function of the distance travelled within the zone. Linear toll functions (i.e. toll charged is proportional to distance traversed) are considered in Zhu and Ukkusuri (2015), Yang et al. (2012), and Gu et al. (2018), and a capped linear distance-based pricing scheme is proposed in Florian and Morosan (2014) wherein minimum and maximum bounds apply on the tolls. A joint distance and time toll is considered by Gu et al. (2018) where drivers are charged jointly in proportion to the distance traveled and time spent within the cordon. In the case of non-linear tolling functions, a key challenge lies in selection/specification of the functional form, an issue that has been addressed by representing the tolling function as a piece-wise linear function of distance (Liu et al., 2014; Meng et al., 2012; Sun et al., 2016).

With regard to model formulation, most distance-based toll optimization problems are formulated as non-linear programs (Yang et al., 2012), bi-level programming models or mathematical programming models with equilibrium constraints (Liu et al., 2014; Meng et al., 2012), and simulation-based optimization problems (Gu et al., 2018). These are solved using a variety of techniques such as meta-heuristics (Meng et al., 2012), reinforcement learning (Zhu and Ukkusuri, 2015), global optimization techniques (Liu et al., 2014), etc. Feeback-control approaches have also been applied in the context of distance-based toll optimization. Gu et al. (2018) propose a solution approach involving the use of a PI-controller to update the toll rate function parameters using estimates of network density. The density estimates are obtained from a network fundamental diagram (NFD) constructed using simulation runs from a Dynamic Traffic Assignment (DTA) model. Along similar lines, Gu and Saberi (2019b) propose a simulation-based optimization (SBO) framework for urban congestion pricing considering travelers' departure time choices. A linear distance-based toll is employed, which is optimized using a discrete proportional-integral (PI) controller to ensure that the NFD of the pricing zone remains in the un-congested regime. Distance-based congestion pricing approaches have also been implemented on idealized networks (Daganzo and Lehe, 2015), at the link level (Simoni et al., 2019), by using nested regions, where only the inner region incurs toll charges, without any consideration of interactions across multiple regions (Gu et al., 2018), and by using nested pricing cordons, where each cordoned zone is priced using piece-wise linear tolling functions (Meng et al., 2012).

Concurrently, while there has been extensive research into partitioning networks based on speed, flow and density data (Gu and Saberi, 2019a; Ji and Geroliminis, 2012; Lentzakis et al., 2014; Saeedmanesh and Geroliminis, 2017) in order to make use of the Network Fundamental Diagram (NFD) concept for traffic network management strategies, including congestion pricing (Geroliminis and Levinson, 2009; Simoni et al., 2015; Zheng et al., 2016, 2012), distance-based pricing has received relatively limited attention in this context.

In summary, in a majority of distance-based pricing-related literature, toll optimization is reactive and based on current network conditions, due to the fact that predictive pricing presents with computational, informational and communication challenges for large-scale networks (de Palma and Lindsey, 2011). Thus, the behavioral responses of the drivers at the future time when the toll is implemented are not taken into account, which may generate inconsistent and sub-optimal tolls. Further, guidance information generation has typically not been integrated into the distanced-based toll optimization formulations. Moreover, existing studies tend to consider only fixed demand and the response of drivers to tolls through lane/route choice (Florian and Morosan, 2014; Yang et al., 2012; Zhu and Ukkusuri, 2015). In contrast, a few works have taken into consideration elastic demand as a function of travel cost (Meng et al., 2012; Sun et al., 2016). However, to the best of our knowledge, there are no studies that have explicitly modeled demand elasticity as a result of drivers behavior in response to distance-based tolling along the dimensions of departure time choice, mode choice, trip cancellation and route choice. Finally, and most importantly, methods for tolling zone definitions in large-scale urban networks to operationalize distance-based tolling schemes have not been systematically examined or assessed in the literature.

This paper attempts to address these gaps by proposing the use of hierarchical density-based clustering methods as a systematic way to help define sets of tolling zones. The objective is to evaluate the impact these systematically derived tolling zone definitions have on network performance, when used as an input to a predictive distance-based toll optimization framework which generates dynamic, predictive road pricing strategies together with traffic guidance. The main contributions of this paper are as follows:

- We propose the use of feature-variant clustering methods for tolling zone definitions in the context of distance-based congestion pricing schemes. In addition to location coordinates, link speeds and link marginal cost tolls based on historical network

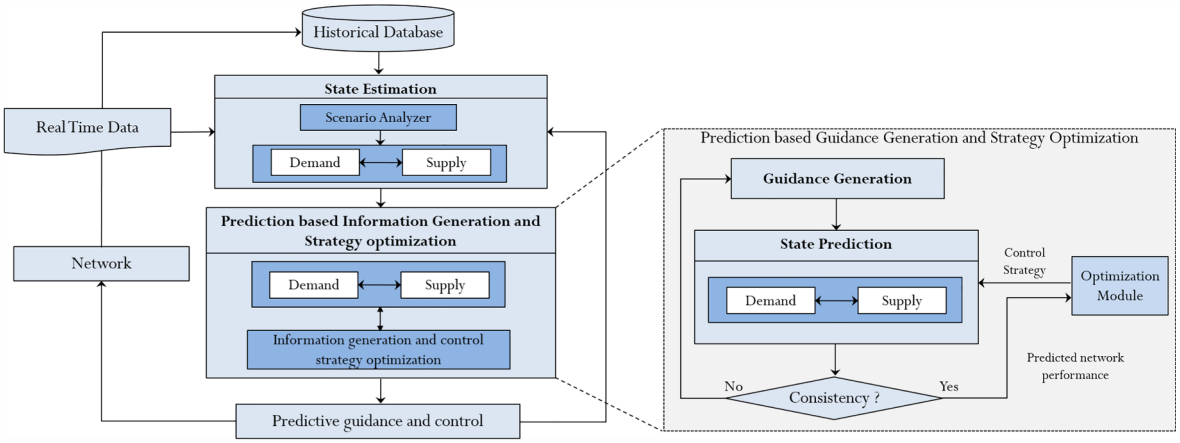

Fig. 1. Framework for Prediction-based Guidance Generation and Distance-based Strategy Optimization.

performance inform the definition of sets of tolling zones for the distance-based tolling optimization application.

- A dynamic distance-based tolling optimization framework is developed utilizing consistent traffic state predictions generated by a simulation-based DTA model within a rolling horizon approach. The framework integrates guidance information generation with toll optimization and explicitly models the behavioral response of users to the distance-based toll charges in terms of mode, route, departure time choices as well as trip cancellation.
- Experiments are conducted on the real-world network of Singapore expressways and major arterial roads under different tolling zone definitions, derived systematically from hierarchical density-based clustering methods, and the optimized distance-based pricing schemes are compared against other popular road pricing schemes, including time-dependent and adaptive cordon-based pricing. Finally, experiments are also conducted on the Boston CBD network to examine performance of the distance-based toll optimization schemes on an urban network.

2. Framework for predictive distance-based toll optimization

The proposed framework for predictive distance-based toll optimization, is shown in Fig. 1 using DynaMIT2.0 - a simulation-based Dynamic Traffic Assignment (DTA) system developed at the MIT Intelligent Transportation Systems Lab (Ben-Akiva et al., 2010; Lu et al., 2015b). It is noted that although the framework is presented using DynaMIT2.0, it can be applied with any real-time simulation-based DTA model system.

DynaMIT2.0 consists two main modules: state estimation and state prediction operating in a rolling horizon scheme. Within a given roll period or execution cycle, the state estimation module integrates real-time data obtained from a traffic surveillance system, historical demand and supply parameters from the historical database, and the distance-based tolling zone definition (described in detail in Section 2) to estimate the current network state through the coupled demand-supply simulators. The state prediction module predicts traffic conditions over the prediction horizon and generates consistent guidance information, which will be disseminated to the travelers during the next roll period.

The control strategy optimization and guidance generation process in DynaMIT2.0 is extended to optimize distance-based tolls. Within this process, the optimization module generates a series of candidate tolling function parameters which are to be evaluated on the basis of a desired objective. The state prediction and guidance generation module takes as input a candidate solution along with an initial guidance and predicts the future network conditions through the coupled demand-supply simulators. This process yields simulated travel times, which will be combined with the previous guidance to generate an updated guidance, and the process continues iteratively until convergence. At this point, the generated guidance is considered consistent and the predicted network performance is used by the optimization module to evaluate the specified objective function. Based on the evaluated objective function value, the optimization module will generate a new set of control strategy candidates and the procedure will continue until optimality or a pre-specified set of termination criteria (e.g. specific time limit, number of iterations) have been achieved.

3. Problem formulation and solution approach

In this section, we describe the optimization problem formulation (based on the framework described in Section 2) including details of the demand model within the DTA system, and the solution approach.

3.1. Context and tolling function definition

The transportation network is represented as a directed graph $G = (N, A)$, where N represents the set of n network nodes and A represents the set of m directed links. Let L be the number of tolling zones in the network G. Each tolling zone l is defined as a subset

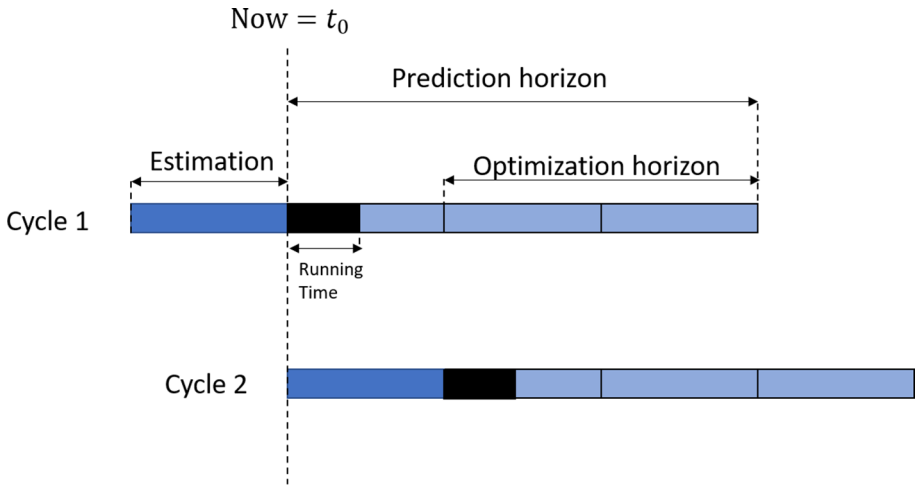

Fig. 2. Rolling Horizon Approach for Tolling Function Optimization.

of A, i.e. $\forall\ l \in \{1,\ ...,L\}$, $A_l \subseteq A$, and is associated with a tolling function $\phi_l(\theta_l^t,\ D_l)$ that maps the distance traveled within zone l, D_l to the toll charge, and θ_l^t is a vector of tolling function parameters in time interval t. The toll payable within any tolling zone is assumed to be bounded, i.e $\tau_{LB} \leqslant \phi_l(\theta_l^t,\ D_l) \leqslant \tau_{UB},\ \forall\ l = 1,\ 2...,L\ \forall\ t = 1,\ 2,\ ...,T$.

Let Δ be the size of the state estimation interval (typically 5 min) and $H\Delta$, the length of the prediction horizon. Without loss of generality, we assume that the optimization horizon (the future period over which we wish to set the tolling function parameters) is the same as the prediction horizon. In addition, assume that the tolling function parameters are fixed over time intervals of size Δ and that the tolling intervals are aligned with the estimation intervals of the DTA system. Consider an arbitrary estimation interval $[t_0 - \Delta,\ t_0]$, let $\theta^h = (\theta_1^h,\ \theta_2^h ... \theta_L^h)$ represent the vector of toll function parameters for all tolling zones for the time period $[t_0 + (h-1)\Delta,\ t_0 + h\Delta]$ where $h = 1,\ ...,H$. The vector of toll function parameters for the current optimization horizon is thus given by $\theta = (\theta^1,\ \theta^2,\ ...,\theta^H)$.

The rolling horizon framework is demonstrated in Fig. 2 with $H = 3$. In execution cycle 1, the decision variables of the optimization problem are the tolling function parameters for the prediction horizon $\theta = (\theta^1,\ \theta^2,\ \theta^3)$. If the optimal values for θ are denoted as $\bar{\theta} = (\bar{\theta}^1,\ \bar{\theta}^2,\ \bar{\theta}^3)$, then the tolling function parameters $\bar{\theta}^1$ are applied in the estimation interval of execution cycle 2 and the procedure repeats. Note that in real-world applications, given the finite running time of the prediction-based optimization, it may not be feasible to implement the optimal tolling function parameters $\bar{\theta}^1$ in the current time interval. In this case, the optimization horizon may be one interval shorter than the prediction horizon, wherein the tolling function parameters for the first sub-interval within the prediction horizon are not optimized and set to optimal values obtained from the previous roll period (or execution cycle).

Further, consider the collection of vehicles $v = 1,\ ...,V$ on the network during the prediction horizon $[t_0,\ t_0 + H\Delta]$. Let the travel time of vehicle v be represented by tt^v and the predictive guidance by $\mathbf{tt}^g = (\mathbf{tt}_i^g\ ;\forall\ i \in A)$, where $\mathbf{tt}^g{}_i$ represents a vector of the time dependent link travel times (guidance) for link i. The vehicle travel times $\mathbf{tt} = (tt^v;v = 1,\ ...,V)$ are the result of the state prediction module of DynaMIT2.0 and thus, cannot be written as an explicit function of the toll function parameters and predictive guidance.

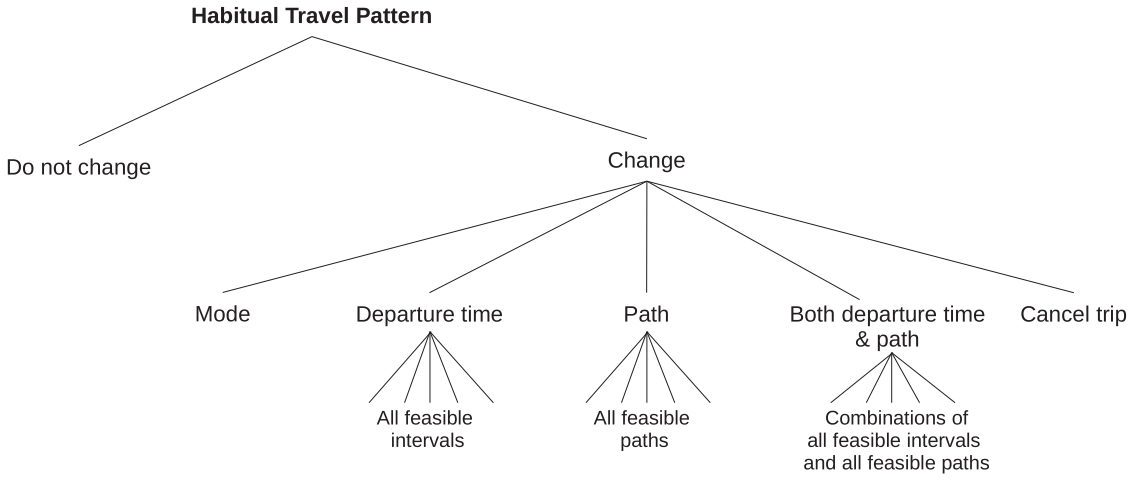

Fig. 3. Pre-trip Behavior Model.

Thus, we characterize the complex relationship through a single constraint that represents the coupled demand and supply simulators of DynaMIT2.0 as:

$$G(\mathbf{x^p}, \gamma^{\mathbf{p}}, \mathbf{tt^g}, \theta) = \mathbf{tt} \tag{1}$$

where $\mathbf{x^p}$, $\gamma^{\mathbf{p}}$ represent the forecasted demand and supply parameters for the prediction horizon, and θ is the vector of tolling function parameters. The iterative procedure within the state prediction module ensures consistency between $\mathbf{tt^g}$ and $\mathbf{tt}$.

3.2. Pre-trip behavioral model with elastic demand

The response of users to the predictive distance-based tolls and travel time guidance is modeled at the pre-trip level. The pre-trip choice model, as illustrated in Fig. 3, includes decisions of trip cancellation, mode, departure time and path and is formulated as a nested logit model.

Thus, a driver may choose to change his/her habitual travel pattern (defined by a habitual route and departure time) in response to the predictive guidance and tolls, in which case he/she may either change mode, cancel trip, change path or departure time, or a combination of the two. With regard to mode choice, the only options we model are to drive or take public transit. The utility of the

Table 1
Pre-trip Behavioral Model - Notation.

Abbreviation	Variable
$ascCM$	Alternative Specific Constant for changing mode
$ascCT$	Alternative Specific Constant for canceling trip
$ascCDT_d$	Alternative Specific Constant for departing at time interval d
c_m^v	money cost for traveling with another mode
c_{dp}^v	distance-based toll for departing at d with path p
t_m^v	travel time when traveling with another mode
t_{dp}^g	predicted travel time for departing at d with path p
$at_{d'p'}^{hab}$	habitual arrival time for departing at habitual departure time interval d' and habitual path p'
at_{dp}^g	predicted arrival time for departing at departure time interval d and path p
β_c^v	coefficient for cost
β_t^v	coefficient for time
β_{early}	coefficient for early arrival
β_{late}	coefficient for late arrival
PS_p	path size variable
C_*	composite utility pertaining to additional variables including path length, number of left turns and number of signalized intersections
ε_*	random error term, i.i.d Gumbel distributed

change mode (CM) alternative for vehicle v is given by (refer Table 1 for notation):

$$\cup^v(CM) = ascCM + \beta_c^v(c_m^v) + \beta_t^v(t_m^v) + \varepsilon_m \tag{2}$$

Unobserved heterogeneity in the valuation of travel time and cost is modeled through a lognormally distributed value of time (more specifically, β_t^v is fixed across individuals whereas β_c^v is computed based on the sampled value of time for individual v). The utility of departing at time interval d and choosing path p for vehicle v is:

$$\begin{aligned}
\cup_{dp}^v \quad &= ascCDT_{dp} + \beta_c^v(c_{dp}^v) + \beta_t^v(t_{dp}^g) \\
&+ \beta_{early}\max(at_{d'p'}^{hab} - at_{dp}^g, 0) + \beta_{late}\max(at_{dp}^g - at_{d'p'}^{hab}, 0) \\
&+ log(PS_p) + C_{dp} + \varepsilon_{dp} \\
&where: \\
c_{dp}^v \quad &= \sum_{l=1}^{L} \phi_l(\vartheta_{p,l}^{t_l}, D_{p,l}^v)
\end{aligned} \tag{3}$$

where t_l is the time at which vehicle v enters zone l. If there is a total of N combinations of path and departure time alternatives in the choice set, the alternative specific constant $ascCDT_{dp}$ can appear in at most $(N-1)$ utilities. The utility of the cancel trip (CT) alternative is:

$$\cup^v(CT) = ascCT + \varepsilon_{CT} \tag{4}$$

The probability of vehicle v choosing alternative c within the choice set C is given by:

$$P^v(c|C) = \frac{e^{\mathscr{V}_c^v/\vartheta}}{\sum_{a\in C} e^{\mathscr{V}_a^v/\vartheta}} \tag{5}$$

where ϑ is the scale parameter and $\not\varepsilon_c^v = \cup_c^v - \varepsilon_c$.

3.3. Optimization formulation

The objective function for the optimization problem can be formulated from the consumers' perspective, producers' perspective or both. In this study, we adopt the objective of total social welfare (SW), defined as the sum of the consumer surplus and the producer surplus. Since we have simulated the choices of each traveler, the consumer surplus (CS) in this setting is simply the sum of the experienced utilities of each traveler. The producer surplus is the net toll revenue (TP) given by the total toll revenue (TR) minus the fixed costs (FC) and variable costs (VC). Thus, $SW = CS + TP = CS + (TR - FC - VC)$. Fixed costs are assumed to be 0, given the fact that optimal tolls are independent of the fixed costs borne by the road operator (Ferrari, 2002). For the computation of total social welfare, the fraction of total toll revenue needed to cover toll operation costs needs to be identified. According to the report in Kirk and Levinson (2016), the cost of operating an electronic road user charge scheme based on distance driven should be minimal and experience in the United States and other countries suggests that the administrative and enforcement costs of collecting user fees would be in the range of 5% to 13% of collections. With this in mind, it is assumed that the toll operation costs are 10% of the total toll revenue. Thus, the variable cost component is assumed to be a portion of the total collected toll revenue with factor $\alpha < 1$. The total social welfare is given by:

$$\begin{aligned} SW &= CS + TP \\ &= CS + (TR - FC - VC) \\ &= \sum_{v=1}^{V} \frac{\cup^v}{|\beta_c^v|} + \left[(1-\alpha) \times \sum_{v=1}^{V} tc^v \right] \end{aligned} \tag{6}$$

The absolute value of β_c^v is used to express the consumer surplus in dollar equivalents. The dynamic distance-based toll optimization problem (DDTOP) in our context is formulated as a non-linear programming problem given in Eq. 7. The decision variables are the vector of tolling function parameters for the optimization horizon period. The objective function is the total social welfare. The constraints are the DynaMIT2.0 system and upper and lower bounds on the toll values.

$$\begin{aligned} &\textbf{DDTOP}: \ \max_{\theta} \left[\sum_{v=1}^{V} \frac{\cup^v}{|\beta_c^v|} + (1-\alpha) \times \sum_{v=1}^{V} tc^v \right] \\ &\textbf{s. t.} \\ &\qquad G(\mathbf{x^p}, \gamma^{\mathbf{p}}, \mathbf{tt^g}, \theta) = \mathbf{tt} \\ &\qquad \tau_{LB} \leqslant \phi_l(\theta_l^h, D_l^v) \leqslant \tau_{UB}, \ \forall\, v = 1, 2, ..., V; l = 1, 2..., L; h = 1, 2, ..., H \end{aligned} \tag{7}$$

Note that in order to prevent drastic changes of the tolling function parameter values across successive estimation intervals, additional constraints may be imposed to restrict the changes across successive intervals within a pre-specified range. These are important considerations in view of acceptability and safety for real-world applications.

3.4. Solution approach

Due to the highly non-linear nature of the objective function of the DDTOP, with no guarantee of concavity, as well as the obvious difficulty to define closed-form analytical expressions that represent the drivers' dynamic route choice decisions as a function of the overall network traffic state and the prevailing tolling strategy, we apply meta-heuristics to solve the optimzation problem formulated in Eq. 7. More specifically, we adopt a real-coded Genetic Algorithm (GA) (Deb et al., 2002) to optimize the parameters of distance-based tolling functions. The GA obviates the need for computationally expensive numerical gradient computations, and is amenable to parallelization, since candidate solutions of the entire population at a given generation can be evaluated in a parallel (see Gupta et al. (2016) for more details).

The algorithm starts with a random population of N control strategy individuals, which form the initial population or parent population. Each control strategy individual is a vector of distance-based toll function parameters for different road pricing zones in the network during the current optimization horizon: $\theta = (\theta^1, \theta^2, ..., \theta^H)$. The Optimization Module passes this population of control strategies to the State Prediction module of DynaMIT2.0 for evaluation based on the predefined objective function. The strategies in the initial population are then ranked based on the values of the objective function (in our case, the total social welfare). From this N-individual parent population, genetic operators (such as tournament selection, SBX crossover, polynomial mutation) are applied to generate another N-individual child population. The newly generated children are then evaluated using the State Prediction module as described previously. After that, they are merged with the parent population to form a larger population of $2N$ individuals out of which, N best individuals are selected to be the parent population for the next generation. The algorithm proceeds iteratively until certain stopping criteria are satisfied. The stopping criteria could be the computational budget in terms of time, the number of generations/iterations or the minimum improvement in the objective function.

In order to speed up the optimization, parallel computing is employed in which the evaluations of different control strategy individuals are conducted in parallel, each in one processing unit, which significantly improves execution time and allows for real-time performance.

4. Clustering approaches for tolling zone definition using OPTICS and HDBSCAN*

The proposed formulation and framework described in Section 3 assume that the tolling zone definitions (in terms of the number of tolling zones and the list of links belonging to each zone) are pre-specified or given. Recall that the tolling function $\phi_l(\theta_l^h, D_l^v)$ is zone specific. Naturally, these zone definitions are likely to significantly affect performance of the distance-based tolling system. To the authors' knowledge, no systematic approach to define distance-based road pricing zones can be found in current research and practice. For our experiments, we originally employed an ad hoc approach to define the tolling zones based on the gantry locations of the cordon-based road pricing system already in operation. In this approach, each distance-based tolling zone corresponds to one gantry and is defined as the area of the network which the vehicles could only access by passing through the gantry. This approach has a similar impact to the drivers' route choice as the gantry system but with added impact of distance to the traveler decisions. While, with this approach, the impact of distance could be directly observed, by comparing the network conditions with cordon-based tolling to the conditions arising from distance-based tolling, it is unsuitable for cases with no pre-existing cordon-based road pricing systems and, most importantly, for large-scale urban network application. To address these shortcomings, we propose the use of clustering methods for tolling zone definition, to be used as an input for the distance-based tolling system.

4.1. Clustering methods

We propose the feature-variant implementation of two well-known hierarchical density-based clustering methods, OPTICS (Ankerst et al., 1999), (Ordering Points To Identify the Clustering Structure), and HDBSCAN* (Campello et al., 2013; McInnes and Healy, 2017), (Hierarchical Density-Based Spatial Clustering of Applications with Noise). While DBSCAN (Schubert et al., 2017), (Density-Based Spatial Clustering of Applications with Noise), is the more established among density-based clustering methods, it is very sensitive to parameter selection and has difficulty in coping with clusters characterized by large inter-cluster density variability. OPTICS and HDBSCAN*, on the other hand, do not suffer from these issues.

OPTICS, like DBSCAN, requires two parameters: ϵ, which describes the maximum distance radius around a particular data point and κ, describing the minimum number of data points used as a density threshold for cluster assignment. Assume $X = \{x_1, x_2, ..., x_n\}$ represents a set of data points in a metric space (X, d). We consider a data point x to be a core point with respect to ϵ and κ if its ϵ-neighborhood $N_\epsilon(x)$ contains a minimum of κ data points. Two core points x_i, x_j are ϵ-reachable with respect to ϵ and κ if they are both contained within each others ϵ-neighborhood. Two core points x_i, x_j are density-connected with respect to ϵ and κ if they are directly or transitively ϵ-reachable. A cluster C, with respect to ϵ and κ, is a non-empty maximal subset of X such that every pair of data points in C is density-connected. This definition of cluster results in the DBSCAN algorithm, upon which both OPTICS and HDBSCAN* are based. OPTICS also considers data points that are part of a more densely packed cluster, so each point is assigned a core distance that describes the distance to the κ-th nearest neighbor:

$$d_{\text{core}}^{\epsilon,\kappa}(x) = \begin{cases} \text{Undefined} & \text{if } |N_\epsilon(x)| < \kappa \\ \kappa\text{-th smallest distance to } N_\epsilon(x) & \text{otherwise} \end{cases} \tag{8}$$

The reachability-distance of data point x_i from data point x_j is either the distance between x_i and x_j, or the core distance of x_i, whichever is bigger:

$$d_{\text{reach}}^{\epsilon,\kappa}(x_i, x_j) = \begin{cases} \text{Undefined} & \text{if } |N_\epsilon(x_i)| < \kappa \\ \max(d_{\text{core}}^{\epsilon,\kappa}(x_i), d(x_i, x_j)) & \text{otherwise} \end{cases} \tag{9}$$

In our OPTICS implementation, we make use of a single global ϵ' value to extract a flat clustering.

HDBSCAN* is essentially the same as OPTICS but with parameter $0 < \epsilon < \infty$, whereas OPTICS simply constrains the range of ϵ. It also employs a different technique to extract a flat clustering, based on the stability of clusters. In the case of HDBSCAN*, we have:

$$d_{\text{core}}^{\kappa}(x_i) = \text{Distance of the } \kappa\text{-th nearest neighbor of } x_i \tag{10}$$

For a given fixed value κ, the mutual reachability distance, derived from the metric d, is defined, as follows:

$$d_{\text{mreach}}^{\kappa}(x_i, x_j) = \begin{cases} \max(d_{\text{core}}^{\kappa}(x_i), d_{\text{core}}^{\kappa}(x_j), d(x_i, x_j)) & \text{if } x_i \neq x_j \\ 0 & \text{if } x_i = x_j \end{cases} \tag{11}$$

HDBSCAN* generates a complete hierarchy of clustering schemes for a range of possible ϵ values, and thus for any fixed ϵ value, the clustering at that level in the hierarchy is going to be the clustering DBSCAN would give for that specific ϵ value. In DBSCAN, only core points belong to clusters. If a point is not a core point it is considered noise and is not assigned to any cluster. Reachability-distance, both in the case of OPTICS and HDBSCAN*, captures this distinction by ensuring a point is not joined into a cluster until the DBSCAN ϵ value is such that the point is within the relevant distance of the other data points in the cluster and the point is a core point at that ϵ value.

While the proposed clustering methods produce clustering schemes where some data points are considered noise, the nature of our problem, tolling zone definition, mandates the assignment of all data points to at least one of the resulting clusters. Therefore, a secondary assignment takes place, whereupon we employ a heuristic that assigns noisy data points to previously assigned data points, based on minimum Euclidean distance.

4.2. Clustering performance metrics

We elected to use two standard internal evaluation indices for the clustering produced by OPTICS and HDBSCAN*, the Silhouette Coefficient (SC) (Rousseeuw, 1987) and the Davies-Bouldin index (DB)(Davies and Bouldin, 1979). In short, SC measures two quantities, cohesion $a(x)$, which measures average distance between data points within the cluster and separation $b(x)$, which measures the minimum average distance of data points to other clusters. Then silhouette $s(x)$ is defined as:

$$s(x) = \frac{b(x) - a(x)}{max\{a(x), b(x)\}} \tag{12}$$

where $s(x) \in [-1, 1]$ takes a value -1 for incorrect clustering, around 0 for overlapping clusters and 1 for highly dense clustering. SC is the average for all data points and can be calculated using:

$$SC = \sum_{i=1}^{N} s(x_i)/N \tag{13}$$

DB is a function of the ratio of intra-cluster scatter to inter-cluster separation. The intra-cluster scatter, S_l, also known as cluster diameter, describes the average of Euclidean distances of each individual data point belonging to cluster C and the cluster centroid. If we define $d_C^{l,m}$ as the inter-cluster centroid distance, then, for number of clusters w, DB can be calculated as follows:

$$\text{DB} = \frac{1}{w} \sum_{l=1}^{w} \max_{l \neq m} \left(\frac{S_l + S_m}{d_C^{l,m}} \right) \tag{14}$$

DB values closer to 0 indicate a better clustering result.

4.3. Clustering results

The network features we opted to use, in addition to location coordinates, are link speed and link marginal cost toll. While speed has often been used as one of the features for spatial clustering of traffic networks (Ji et al., 2014), marginal cost toll has not been considered before as a feature. Marginal cost tolls have been used at the link level for first-best toll pricing studies. For large road networks, calculating marginal cost tolls for individual links, at each time interval, can be extremely onerous, which limits the potential for real-time large-scale practical applications (de Palma and Lindsey, 2011). One way to address this limitation is to use the average marginal cost tolls for each link over a period of time, such as morning or evening peak period, given the fact that traffic conditions during peak periods follow recurrent patterns (Small and Verhoef, 2007). Our innovation lies in the fact that we make use of link marginal cost tolls, averaged over a predetermined period, which inform the definition of appropriate tolling zones for distance-based tolling optimization application, rather than calculating tolls for each link throughout the peak period. This allows for the practical implementation of our distance-based tolling optimization approach on large-scale road networks. Our main considerations in using the average were twofold. First, since the tolling zones are pre-specified and fixed for the entire simulation period (time period of interest), we needed a single representative value of the marginal cost toll for a given link during the clustering process. In view of this requirement, we used the average of marginal cost tolls across five minute intervals rather than the marginal cost tolls for the entire simulation period (computed based on average flows and speeds), since the former better captures the dynamics of the marginal cost toll variation.

The link flow-speed-density relationship used in DynaMIT2.0 is as follows (note that for simplicity in the computation of the marginal cost tolls, we consider only the moving part of the link/segment where vehicle movement is dictated by a modified Greenshields (Ben-Akiva et al., 2010) model):

$$q = k \cdot v_f \left[1 - \left(\frac{k}{k_{jam}} \right)^{\chi} \right]^{\psi} \tag{15}$$

where χ, ψ are model parameters and q, v_f, k, k_{jam} represent flow, free flow speed, density and jam density respectively. The marginal cost toll for link i (for simplicity we omit the subscript i in all terms) is given by de Palma and Lindsey (2011):

$$\delta = \gamma q \cdot \left(\frac{dt}{dq} \right) \tag{16}$$

where γ represents the average value of time of vehicles traversing link i. Assuming s represents link length, from Eqs. 15 and 16 we have:

$$\delta = \gamma \left(\frac{-q \cdot s}{v^2} \right) \cdot \left(\frac{\chi\psi \left(\left(\frac{v}{v_f} \right)^{1/\psi} - 1 \right)}{k_{jam} \left(1 - \left(\frac{v}{v_f} \right)^{1/\psi} \right)^{1/\chi} \left(\chi\psi \left(\frac{v}{v_f} \right)^{1/\psi} - \chi\psi + \left(\frac{v}{v_f} \right)^{1/\psi} \right)} \right) \tag{17}$$

It should be pointed out that in case of more complex urban networks, queuing delays should be considered in the computation of the

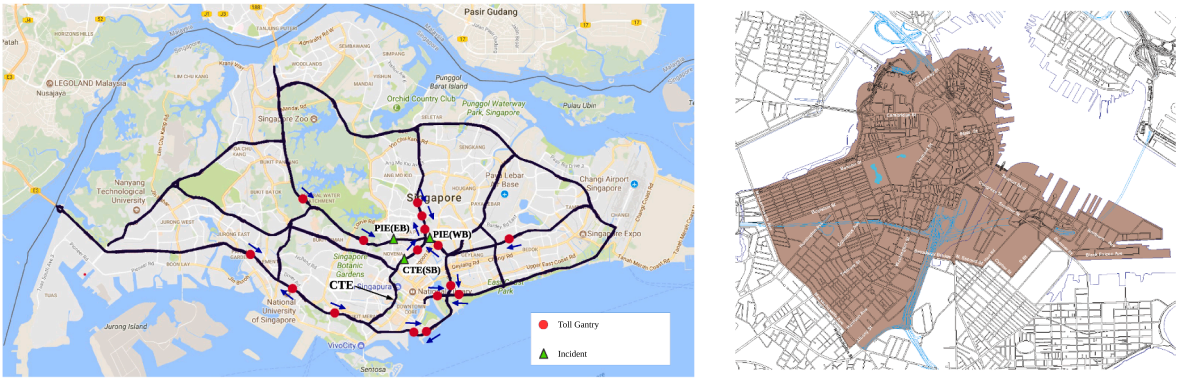

(a) Singapore Expressways and Major Arterials Network

(b) Boston CBD Network

Fig. 4. Test Case Networks.

marginal cost tolls (see Yang and Huang (1998)).

Certain requirements have to be met, in order to guarantee low computational overhead, feasibility and ultimately, practical application potential of this framework. First and foremost, the number of tolling zones has to be kept low, to allow for feasible practical implementation. All resulting clusters must be spatially compact, i.e., not have links in completely disparate locations belong to the same cluster. Tolling zone definitions may not change throughout the simulation horizon, to limit computational overhead and subsequently ensure the feasibility of a practical implementation for large-scale networks.

The data used for clustering include simulated speeds and densities at the link and segment level (for the morning peak period) obtained from a calibrated DynaMIT2.0 model of the Singapore Expressways and Major Arterial Roads network shown in Fig. 4a, as well as a calibrated model of the Boston Central Business District, shown in Fig. 4b. The Singapore network has 939 nodes, 1157 links, 3906 segments, 10954 lanes and 4120 Origin-Destination pairs. The Boston CBD network has 846 nodes, 1746 links, 3085 segments, 5057 lanes and 13080 Origin-Destination pairs. More details of the offline calibration process to determine historical demand and supply parameters (dynamic origin-destination demands, segment capacities and traffic dynamics parameters, route choice parameters) may be found in Gupta et al. (2020) and Lu et al. (2015a). The rationale for using simulated data as opposed to observed data is the limited spatial coverage (in terms of fraction of network links) of available traffic data for the network and the presence of noisy measurements.

After taking into consideration the requirements described above, with careful parameter tuning, we were able to acquire appropriate tolling zone definitions for the Singapore and Boston networks. For the Singapore network, 4 tolling zone definitions were generated, 2 using the link speed feature (obtained directly from simulated measurements), referred to as SPD, and 2 using the average link marginal cost toll feature (computed using Eq. 17 based on simulated speeds and flows), referred to as MCT, for OPTICS and HDBSCAN* respectively. In contrast, for the Boston network, 2 tolling zone definitions were generated, using the average link marginal cost toll (MCT) feature (computed using Eq. 17 based on simulated speeds and flows), for OPTICS and HDBSCAN* respectively. Interestingly, in the case of the Boston network, clustering results derived from MCT and SPD yield identical tolling zone definitions for both OPTICS and HDBSCAN* (hence, only MCT is reported both in this Section as well in Section 6). This may be attributed to the fact that while the correlation for the normalized SPD and MCT feature datasets from the Singapore network was found to be moderate, in case of the Boston network they were found to be strongly correlated. However, this may be a peculiar feature of the Boston CBD network, and more investigation on other urban networks is required to gain more insight into this relationship. The tolling zone definitions for each clustering method and feature, as well as the clustering performance index results, are presented in Figs. 5–7. Note that each color represents a separate cluster or zone. The qualitative differences between these zone definitions using the different clustering methods are discussed in Section 5.2.

5. Experiments: Singapore expressway network

5.1. Experimental design

In order to investigate the impact tolling zone definitions –which are derived from feature-variant clustering methods– have on the performance of adaptive distance-based congestion pricing schemes, when applied on an expressway and arterial network, experiments are conducted on the Singapore network illustrated in Fig. 4a. A linear tolling function is considered with lower and upper bounds on the toll charged in each zone (i.e $\phi_l(\theta_l^t, D_l) = \theta_{l1}^t + \theta_{l2}^t D_l$; and $0 \leqslant \phi_l(\theta_l^t, D_l) \leqslant 3$). The simulation period is from 07:00 to 11:00 covering the morning peak. As noted earlier, historical demand and supply parameters are obtained from prior offline calibrations of DynaMIT2.0 for the Singapore expressway and arterial network (Gupta et al., 2020; Lu et al., 2015a). The estimation interval is 5 min and the prediction horizon is 30 min. Moreover, 3 incidents from the historical database of Land Transport Authority of Singapore are included to examine the robustness of the tolling zone definitions (which are based on network performance on an

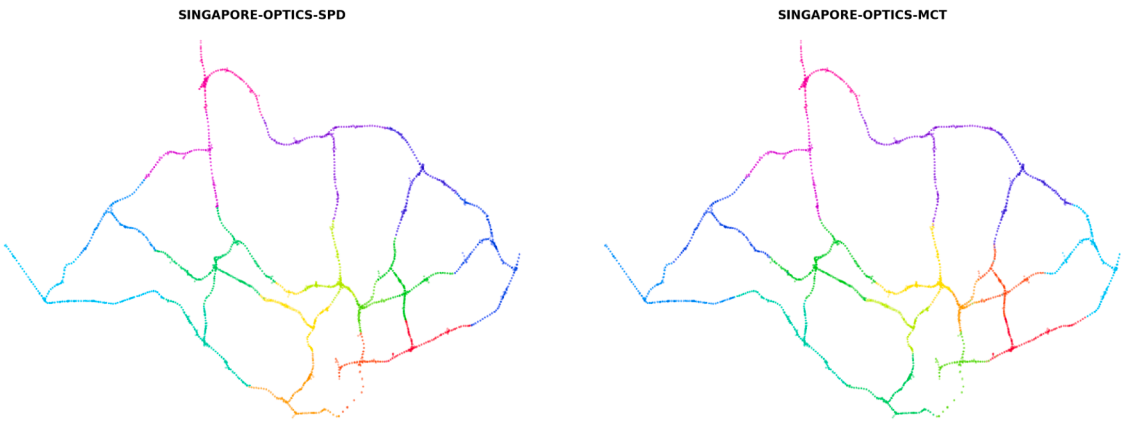

(a) 16 zones derived using OPTICS for feature SPD, with SC=0.430, DB=0.775

(b) 16 zones derived using OPTICS for feature MCT, with SC=0.412, DB=0.798

Fig. 5. Tolling zone definitions and clustering performance results from using OPTICS (each color represents an individual cluster or zone).

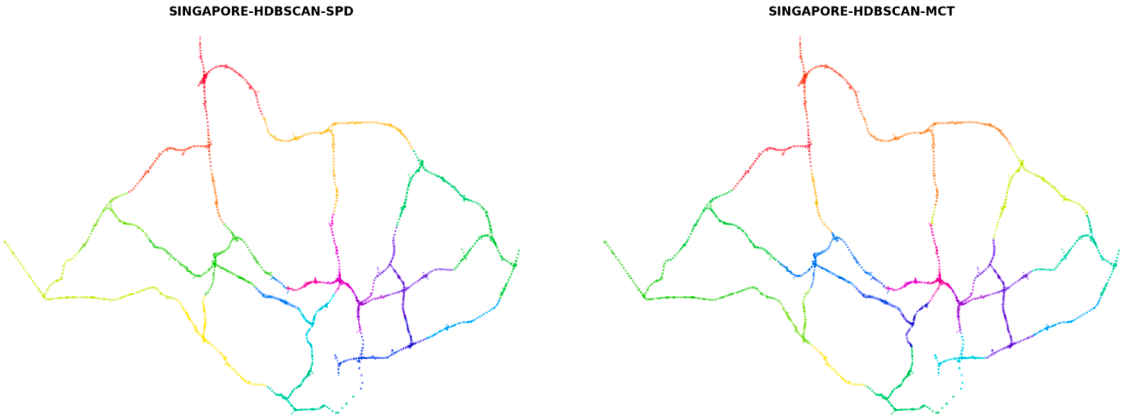

(a) 20 zones derived using HDBSCAN* for feature SPD, with SC=0.394, DB=0.744

(b) 20 zones derived using HDBSCAN* for feature MCT, with SC=0.393, DB=0.756

Fig. 6. Tolling zone definitions and clustering performance results from using HDBSCAN* (each color represents an individual cluster or zone).

average day) to non-recurrent events. The selected incidents include 2 major incidents on the Pan Island Expressway (East Bound and West Bound) and one major incident on the Central Expressway (South Bound) as also shown in Fig. 4a.

The coefficients of the choice model were obtained by calibrating a previously estimated model using aggregate traffic count data, and the calibrated parameter values are summarized in Appendix A. The mean value of travel time is S$23.5, which is similar to that observed in the literature for car drivers in Singapore (Li et al., 2011), and the standard deviation is S$5.75.

Since the objective function is total welfare, comparisons across scenarios (or tolling schemes) are only meaningful for a specific population of travelers including the individuals who cancel or change mode. Therefore, performance measures are calculated for the population of vehicles with habitual departure time within 07:00–10:00 (these drivers may later change the departure time in response to the traffic conditions). A *warm-up* period of 1 h (06:00–07:00) is used, and the last one hour of simulation (10:00–11:00) is a *cool-down* period without toll optimization to ensure that all the vehicles with habitual departure time in 07:00–10:00 finish their trips. A total of seven models or scenarios are considered, which are summarized in Table 2. All scenarios involve dynamic or time-dependent tolls, and with the exception of the base scenario (S0), are optimized predictive tolls computed using the framework described in Section 2. Recall that the state estimation interval is 5 min implying that in the case of cordon-based pricing schemes the toll rates vary every 5 min, whereas in the case of distance-based pricing schemes the tolling function parameters vary every 5 min.

The base scenario **S0** includes a **time-dependent cordon-based pricing** scheme that is currently in operation in Singapore (also called ERP or Electronic Road Pricing). The tolls for this scenario are based on the real toll rates of the Singapore Expressway Network including 16 gantries, whose location is illustrated in Fig. 4a. The first scenario **S1** is **adaptive cordon-based pricing** in which, tolls for fixed gantry locations are dynamically optimized based on state predictions within the framework described in Section 2 (more

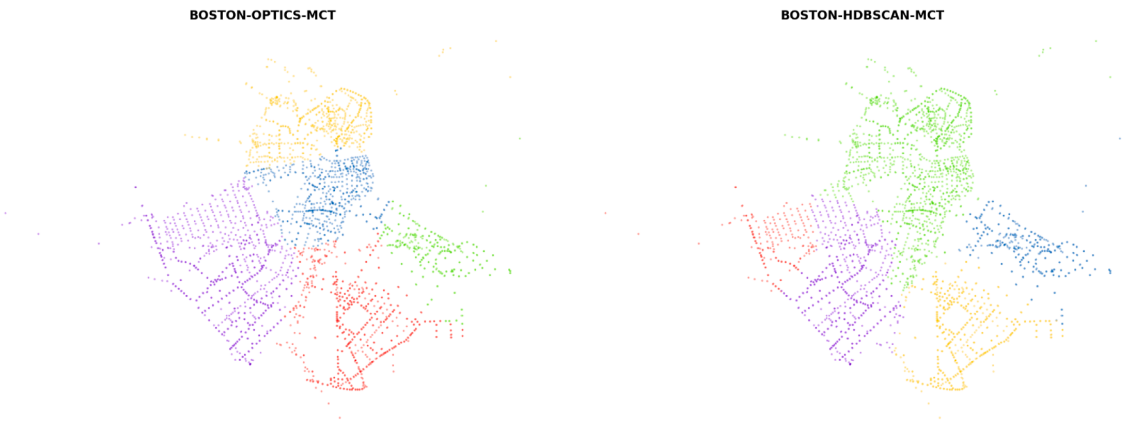

(a) 5 zones derived using OPTICS for feature MCT, with SC=0.388 DB=0.858

(b) 5 zones derived using HDBSCAN* for feature MCT, with SC=0.400, DB=0.776

Fig. 7. Tolling zone definitions and clustering performance results from using OPTICS and HDBSCAN* (each color represents an individual cluster or zone).

Table 2
Summary of Singapore network simulation scenarios.

Scenario	Tolling Scheme	Description
S0	Cordon-based	*Non-adaptive*, based on real toll rates
S1	Cordon-based	*Adaptive*, optimized predictive tolls for fixed gantries
S2	Distance-based	*Optimized predictive: ad hoc*
S3	Distance-based	*Optimized predictive: OPTICS-SPD*
S4	Distance-based	*Optimized predictive: OPTICS-MCT*
S5	Distance-based	*Optimized predictive: HDBSCAN*-SPD*
S6	Distance-based	*Optimized predictive: HDBSCAN*-MCT*

details on the exact formulation may be found in Gupta et al. (2016)).

Scenarios **S2**-**S6** are variants of the predictive distance-based tolling scheme (Section 3) that differ solely in the definitions of the tolling zones. In scenario **S2** (termed **ad hoc**), the tolling zone definitions are derived in an **ad hoc** manner, using the fixed gantry locations as a starting point and containing the area of the network which the vehicles could only access by passing through each gantry. The third scenario **S3** (termed **OPTICS-SPD**) involves tolling zone definitions derived from the clusters obtained based on speed data using OPTICS. In scenario **S4** (termed **OPTICS-MCT**), the tolling zone definitions are derived from MCT data using OPTICS. The fifth scenario **S5** (termed **HDBSCAN*-SPD**), involves tolling zone definitions derived from speed data using HDBSCAN*. In the sixth scenario **S6** (termed **HDBSCAN*-MCT**), tolling zone definitions are derived from MCT data using HDBSCAN*. Finally, two additional scenarios, **S7** and **S8** —which involve tolling zone definitions derived from a combination of speed and marginal costs tolls— are discussed in Appendix C.

The performance of the various tolling schemes (scenarios **S0**-**S6**) is evaluated on the basis of the objective function, which is to maximize the total social welfare (SW). In addition, other performance measures such as the consumer surplus (CS), tolls charged, and average travel time (TT) are also examined to observe the impact on individual travelers, in terms of overall benefit, monetary cost and travel time respectively.

5.2. Results

The performance measures in terms of SW, CS and TT for all scenarios are summarized in Table 3. Furthermore, the differences in SW and CS (in $ amounts) of scenarios **S1**-**S6** relative to the base scenario S0 are shown in Fig. 8a (percentage differences are not meaningful in case of SW and CS which are defined only up to an additive constant). The performance improvement in terms of average travel time (%) over the base scenario S0 is illustrated in Fig. 8b.

As is evident from the results, as expected, all the adaptive tolling schemes yield an improvement in overall social welfare and consumer surplus relative to the existing non-adaptive cordon-based scheme currently in operation. The improvements in social welfare and consumer surplus range between S$106780 - S$510405 and S$12814.3 - S$256896. The large variation of differences in SW and CS confirms that the definition of the tolling zones does play a significant role in the performance of the distance-based tolling scheme. In terms of average SW per traveller, the maximum improvements of an adaptive distance-based tolling scheme relative to an adaptive cordon-based scheme (**S6** vs **S1**) are around S$ 1.275. These significant improvements in welfare can be

Table 3
Performance metrics SW, CS and TT for **S1**, **S2**, **S3**, **S4**, **S5**, **S6**.

	Scenarios					
Metrics	*S*1	*S*2	*S*3	*S*4	*S*5	*S*6
SW ($)	106780.8	241119.1	139581.9	505341.3	235575.3	510405.3
CS ($)	76793.8	146989.7	12814.3	250802.7	30317.2	256896.2
TT (s)	586.3	564.6	577.8	511.2	559.4	512.5

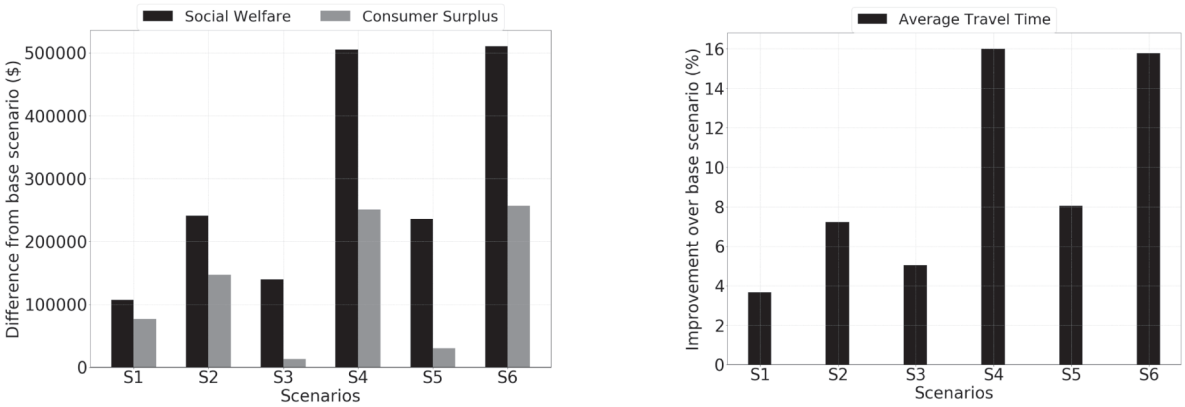

(a) Difference in SW, CS for scenarios **S1-S6** relative to **S0**

(b) Percentage Improvement in TT for scenarios **S1-S6** relative to **S0**

Fig. 8. Percentage results for scenarios **S1-S6** relative to **S0**.

attributed to the improved efficiency of the distance-based tolling schemes (especially in the presence of non-recurrent events) leading to larger reductions in travel times and schedule delays, notwithstanding the higher toll charges.

With regard to the impact of the tolling zone definitions and the clustering methods, both OPTICS and HDBSCAN* produce clustering results with significantly higher impact on the performance of distance-based toll optimization when the marginal cost tolls are used rather than speeds (**S4, S6** which yield the largest SW improvements of over S$500000). These results are intuitive and can be explained by the fact that link marginal cost tolls contain more information regarding traffic externalities and employ the slope of congestion cost function of each link, allowing a more efficient internalization of these costs with distance-based tolling. In our context, the difference between speed and MCTs manifests in the southern part of the network (the Central Business District) where the use of speeds results in certain clusters having a combination of both arterials and expressways, which is not the case when MCTs are used for clustering. Thus, the results suggest that if accurate estimates of the marginal congestion costs can be derived at the link level, these may be better suited than link speeds or densities to inform the definitions of tolling zones.

Moreover, interestingly, in the case of OPTICS, the use of speed as a feature yields a significantly poorer performance in terms of social welfare (and travel time improvement) than the ad hoc zone definitions (**S2** vs **S3**). It is plausible that the existing gantry locations (on which the ad hoc zone definitions are based) already capture well the spatial patterns of congestion. The number of zones may also play a role, although the impact of this requires more systematic investigation, and has implications on the complexity of the optimization.

In terms of average travel times, the distance-based tolling schemes using MCT (**S4** and **S6**) yield the largest improvements of around 16% (relative to **S0**). These significant improvements in travel times (and consequently schedule delay) are the primary reason for the higher social welfare as described previously. Further, using a higher number of zones does not necessarily guarantee improved performance as can be observed in scenario **S2** versus **S5**. **S2**, based on the ad hoc zone definitions (16 in number) yields a marginally higher SW compared to the HDBSCAN* (20 zones). However, the differences in terms of CS are significant (**S2** is significantly higher), which can be attributed to higher toll charges in **S5** where every network link is assigned to a zone, and hence is tolled. This is not the case for **S2**, resulting in fewer travelers being charged, and for shorter distances.

In Fig. 9a, the Empirical Cumulative Distribution Function (ECDF) of the total toll charge (for the population of vehicles) for all scenarios is presented (refer Appendix B for more details on the distribution). It is evident that the majority of the traveler population (around 85%) pay $0 in the case of the cordon-based pricing schemes (scenarios **S0** and **S1**). Moreover, the ECDF for the cordon-based schemes is discontinuous owing to the fact that only certain routes during certain time periods are tolled, in contrast with the more continuous ECDF for the distance-based tolling schemes. Further, the overall magnitude of toll charges (as well as the % of users

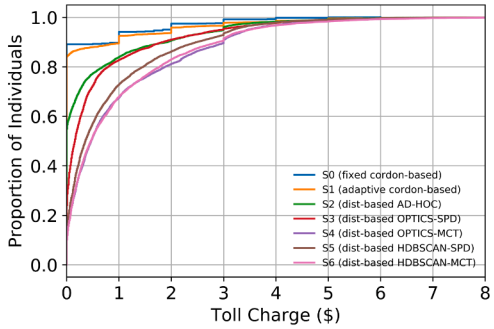

(a) ECDF of total Toll Charge values for scenarios **S0-S6**

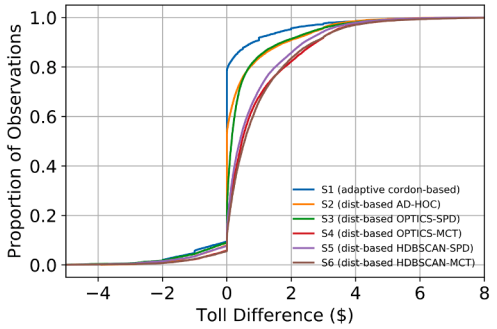

(b) ECDF of difference in total Toll Charge per OD-pair for scenarios **S1-S6** relative to **S0**

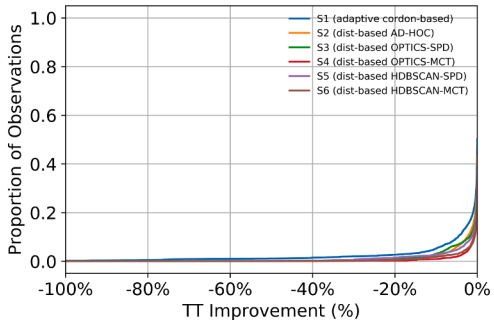

(c) ECDF of TT improvement per OD-pair over **S0** for scenarios **S1-S6** (*negative*)

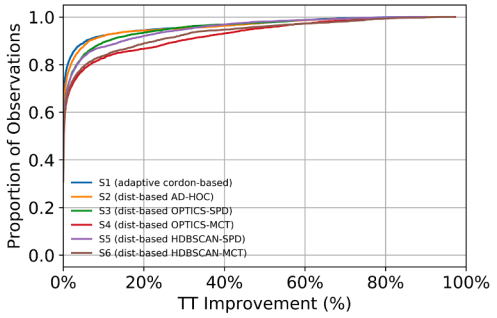

(d) ECDF of TT improvement per OD-pair over **S0** for scenarios **S1-S6** (*positive*)

Fig. 9. Empirical Cumulative Distribution Functions for scenarios **S1-S6** relative to **S0**.

tolled) in the case of distance-based tolling is higher, with the highest total charges observed in case of **S4** and **S6**, which incidentally, happen to be the best performing scenarios. Thus, despite the higher toll charges in case of distance-based tolling, the significant improvements in travel time and schedule delays lead to improved consumer surplus, with tolling zone definitions derived from MCT (both with OPTICS and HDBSCAN*) resulting in more efficient tolling, and hence, the best performance in terms of SW, CS and TT.

In order to analyze the impact of distance-based tolling in more detail from the travelers' perspective, the Empirical Cumulative Distribution Function (ECDF) of the difference in toll charge, as well as travel time improvement relative to the base scenario **S0** at the level of the individual traveler, are presented in Fig. 9b, c and d respectively (the corresponding kernel density functions are shown in Figs. 13 and 12 in Appendix B). As is evident from Fig. 9c, d, almost 40% of the traveler population experience similar travel times for all scenarios (compared to the base scenario). For about 25% of the traveler population, travel times are higher (by up to 80%) for **S1** and up to 30% for all scenarios employing distance-based tolling methods (S2-S6), compared to base scenario **S0**. Concretely, for about 35% of the traveler population, travel times are lower by up to 85% for S4 and S6, the best performing scenarios, and up to 75% for all remaining scenarios (**S2, S3, S5**). These are particularly OD-pairs affected by the incidents. It is also evident that the largest proportion of the traveler population subset that benefits from lower travel times corresponds to **S4**, followed closely by **S6**.

Finally, regarding the difference in toll charges paid by the travelers, compared to the base scenario **S0**, it is evident from Fig. 9b that, for only 10% of the population, the adaptive toll charges in scenario **S1** are lower than that of the base scenario **S0**. Similarly, the corresponding proportions for the distance-based tolling schemes (**S2-S6**) range from about 7% to 9%. In case of the adaptive cordon-pricing scheme (**S1**), almost 70% of the population pays an equal toll charge as that in **S0** (most of these are zero tolls as noted in Fig. 9a). The corresponding population proportion for **S2** is about 45%, decreasing further to about 15% for **S3** and ranging from 8%-12% for **S4,S5** and **S6**. The remaining populations for all scenarios (approximately 20% for **S1**, 45% for **S2**, 75% for **S3**, 85% for **S4,S5,S6**) pay a higher toll charge than that of the population in the base scenario **S0**. These corroborate the previously discussed findings that in general, the distance-based tolling schemes result in higher tolls per traveler, and a more efficient tolling based on network utilization, thus leading to significant improvements in social welfare and network performance.

Table 4
Summary of Boston network simulation scenarios.

Scenario	Tolling Scheme	Description
B0	No Toll	–
B1	Distance-based	*Optimized predictive: OPTICS-MCT*
B2	Distance-based	*Optimized predictive: HDBSCAN*-MCT*

6. Experiments: boston CBD network

6.1. Experimental design

In order to investigate the impact tolling zone definitions –which are derived from feature-variant clustering methods– have on the performance of adaptive distance-based congestion pricing schemes, when applied on an urban network, experiments are conducted on the Boston CBD network illustrated in Fig. 4b. As with the Singapore network, a linear tolling function is considered with lower and upper bounds on the toll charged in each zone (i.e $\phi_l(\theta_l^t, D_l) = \theta_{l1}^t + \theta_{l2}^t D_l$; and $0 \leqslant \phi_l(\theta_l^t, D_l) \leqslant 1.5$). Given the smaller zones (in terms of area) and shorter average link length, we adjusted the toll cap appropriately. The simulation period is from 06:00 to 09:00 covering the morning peak. As noted earlier, historical demand and supply parameters are obtained from prior offline calibrations of DynaMIT2.0 for the Boston Central Business District network (Azevedo et al., 2018). The estimation interval is 5 min and the prediction horizon is 30 min.

The performance measures are calculated for the population of vehicles with habitual departure time within 06:00–09:00 (these drivers may later change the departure time in response to the traffic conditions). As compared to the Singapore network, a shorter *warm-up* period of 15 min is used and the last 15 min of the simulation is a *cool-down* period without toll optimization to ensure that all the vehicles with habitual departure time in 06:00–09:00 finish their trips. A total of three scenarios are considered, which are summarized in Table 4. All scenarios involve dynamic tolls computed using the framework described in Section 2, with the exception of the base scenario (B0) which is the *No Toll* case. Recall that the state estimation interval is 5 min implying that in the case of distance-based pricing schemes the tolling function parameters vary every 5 min.

The base scenario **B0** is set up to reflect traffic conditions in the Boston Central Business District without any tolling scheme in place. The first and second scenarios **B1**, **B2** are variants of the predictive distance-based tolling scheme (Section 3) that differ solely in the definitions of the tolling zones. In scenario **B1** (termed **OPTICS-MCT**), the tolling zone definitions are derived from MCT data using OPTICS. The second scenario **B2** (termed **HDBSCAN*-MCT**), involves tolling zone definitions derived from MCT data using HDBSCAN*.

Similar to the Singapore network, the performance of scenarios **B0**-**B2** is evaluated on the basis of the objective function, which is to maximize the total social welfare (SW). In addition, other performance measures such as the consumer surplus (CS), tolls charged, and average travel time (TT) are also examined to observe the impact on individual travelers, in terms of overall benefit, monetary cost and travel time respectively.

6.2. Results

The performance measures in terms of SW, CS and TT for all scenarios are summarized in Table 5. Furthermore, the differences in SW and CS (in $ amounts) of scenarios **B1, B2** relative to the base scenario B0 are shown in Fig. 10a. The performance improvement in terms of average travel time (%) over the base scenario B0 is illustrated in Fig. 10b.

As is evident from the results, as expected, all the adaptive tolling schemes yield an improvement in overall social welfare and consumer surplus relative to the existing scheme with no tolls currently in operation. The improvements in social welfare and consumer surplus range between $179285.0 - $194032.6 and $84083.7 - $127062.4. In terms of average SW per traveller, the maximum improvements of an adaptive distance-based tolling scheme relative to the no toll case (**B2** vs **B0**) are around $2.15. Larger variation of differences in CS confirms that the definition of the tolling zones does play a significant role in the performance of the distance-based tolling scheme. These significant improvements in welfare can be attributed to the efficiency of the distance-based tolling schemes leading to significant reductions in travel times and schedule delays, notwithstanding the presence of toll charges.

With regard to the impact of the tolling zone definitions and the clustering methods, both OPTICS and HDBSCAN* produce clustering results with significant positive impact on network performance when compared to the no toll scenario, with HDBSCAN*-

Table 5
Performance metrics SW, CS and TT for **B1**, **B2**.

	Scenarios	
Metrics	**B1**	**B2**
SW ($)	179285.0	194032.6
CS ($)	84083.7	127062.4
TT (s)	166.9	157.1

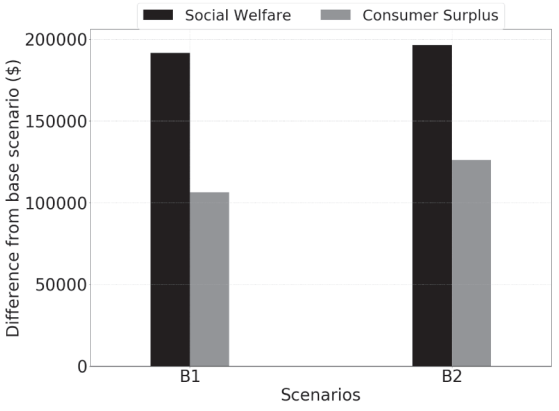

(a) Difference in SW, CS for scenarios **B1, B2** relative to **B0**

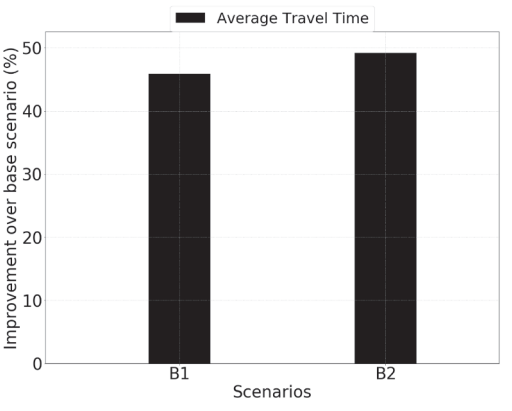

(b) Percentage Improvement in TT for scenarios **B1, B2** relative to **B0**

Fig. 10. Performance results for scenarios **B1**, **B2** relative to **B0**.

derived tolling zone definition having the highest impact on distance-based tolling optimization performance, similar to the Singapore network.

In terms of average travel times, the distance-based tolling schemes yield large improvements of up to 49% (relative to **B0**). It should be noted that these improvements are over a no toll base scenario, not a pre-existing cordon-based tolling scheme, as is the case for the Singapore network. These significant improvements in travel times (and consequently schedule delay) are the primary reason for the higher social welfare as described previously.

Concretely, the difference in improvement, when compared to the Singapore network results, may be attributed to more congestion, the significantly larger number of route alternatives in the Boston CBD network as well as the nature of demand (given it is a sub-network, there are a large number of internal-external and external-internal trips of short length). Additionally, it should be noted that, the Boston network is an urban traffic network with shorter links, fewer lanes per link and traffic patterns characterized by lower average speed and traffic flow interruptions due to the traffic signal infrastructure.

In Fig. 11a, the Empirical Cumulative Distribution Function (ECDF) of the total toll charge (for the population of vehicles) for scenarios **B1, B2** is presented. It is evident that the majority of the traveler population (almost 80%) pay total tolls no higher than $3 for both distance-based pricing schemes. Further, the overall magnitude of toll charges in the case of scenario **B1** is consistently higher than that of scenario **B2**, which happens to be the best performing scenario. It should be noted that, despite the presence of toll charges in the case of each distance-based tolling scheme, the significant improvements in travel time and schedule delays lead to improved consumer surplus and hence, the best performance in terms of SW, CS and TT.

In order to analyze the impact of distance-based tolling in more detail from the travelers' perspective, the Empirical Cumulative Distribution Function (ECDF) of travel time improvement, as well as the difference in toll charge relative to the base scenario **B0** at the level of the individual traveler, are presented in Fig. 11b.

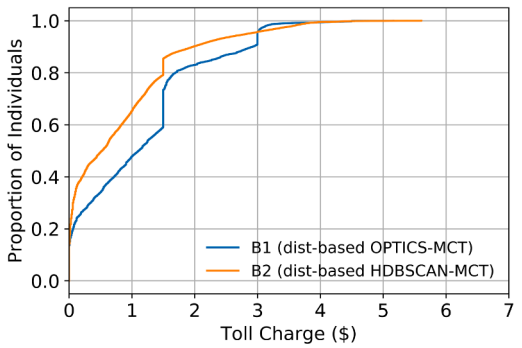

(a) ECDF of total Toll Charge values for scenarios **B1, B2**

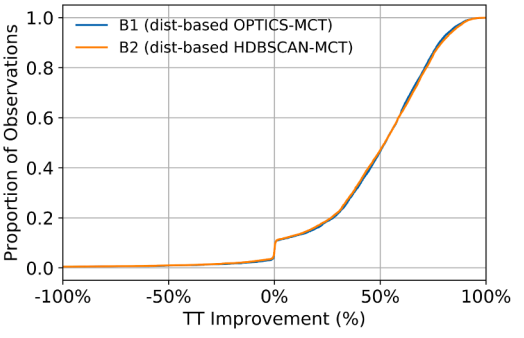

(b) ECDF of TT improvement per OD-pair over **B0** for scenarios **B1, B2**

Fig. 11. Empirical Cumulative Distribution Functions for scenarios **B1**, **B2** relative to **B0**.

As is evident from Fig. 11b, for less than 10% of the traveler population, travel times are equal or lower for scenario **B0**, as compared to scenarios **B1, B2**. Up to 90% of the traveler population benefits from lower travel times, in both scenarios **B1, B2** employing distance-based tolling methods, compared to base scenario **B0**. It is also evident that the largest proportion of the traveler population subset that benefits from lower travel times corresponds to **B2**, though followed very closely by **B1**.

Due to the lack of a pre-existing tolling scheme to be used as a base case, unlike the Singapore network, we cannot corroborate the previously discussed findings relating to comparisons against a cordon-based scheme (distance-based tolling schemes result in higher tolls per traveler, and a more efficient tolling based on network utilization). Nevertheless, compared to our no toll base case, we observed very significant improvement, both in social welfare and network performance, which suggests that the clustering methods can yield effective definitions of tolling zones for application of distance-based pricing schemes to urban networks as well.

7. Conclusions and future work

In this paper, we propose the use of feature-variant hierarchical density-based clustering methods to systematically define tolling zones for distance-based pricing schemes, and examine the impact of these tolling zone definitions on traffic network performance, when used as input within a predictive distance-based toll optimization framework. The proposed distance-based toll optimization framework integrates consistent guidance generation with the predictive optimization of tolling function parameters for the distance-based pricing scheme. We evaluated this framework's performance against other popular road pricing schemes, including adaptive cordon-based pricing, on the real-world Expressways and Major Arterials network of Singapore. Due to the significant differences between expressway and urban networks, in terms of topology and traffic dynamics, we decided to further investigate this framework's performance on the real-world urban network of the Boston Central Business District. For the Singapore network, results indicate that the best performance in terms of social welfare and network performance comes from the use of a tolling zone definition derived from link marginal cost tolls (MCT), using OPTICS and HDBSCAN*. It should be noted that, while clustering performance evaluation results (SC, DB) are a good indicator of tolling optimization performance improvement, other factors, such as the type of feature used in deriving tolling zone definitions, may play a deciding role. For instance, when using a tolling zone definition derived from link speed data (SPD), using HDBSCAN*, performance was better than time-dependent and adaptive cordon-based pricing schemes and comparable to that of a tolling zone definition derived in an ad hoc manner. When using a tolling zone definition derived from link speed data (SPD), using OPTICS, performance was better than time-dependent and adaptive cordon-based pricing schemes and significantly worse than that of a tolling zone definition derived in an ad hoc manner. This warrants further investigation, although in general, HDBSCAN* has proven to be more robust in providing a tolling zone definition, which, when used as input to our predictive distance-based toll optimization framework, has a positive impact on social welfare and network performance. This conclusion is further corroborated by the results for the Boston network, where the HDBSCAN*-derived tolling zone definition had the most positive impact, on social welfare. While we were able to get very good performance from the use of a tolling zone definition derived from link marginal cost tolls (MCT), using both OPTICS and HDBSCAN*, in a practical implementation, OPTICS may be preferable, given the fact that the higher number of tolling zones in the tolling zone definition derived using HDBSCAN* (20) would introduce an additional computational overhead to the predictive distance-based toll optimization. In conclusion, all factors considered, OPTICS using marginal costs tolls as a clustering feature appears to be a suitable choice to systematically derive a tolling zone definition for the Singapore network. For the Boston network, the number of zones for each tolling zone definition derived from OPTICS and HDBSCAN*, respectively, is identical (5). In this case, HDBSCAN* is clearly the superior clustering method, with significant benefits to tolling optimization when compared to OPTICS. Having said this, network topology and spatio-temporal patterns of demand and congestion are likely to play an important role, and more tests are required in different contexts to further examine the robustness of the methodology.

In future work, we aim to investigate the possibility of implementing OPTICS and HDBSCAN*, as well as other appropriate clustering algorithms, to define sets of tolling zones on data sets from full-scale urban networks such as the greater Boston area or the Singapore urban network, with additional features (density, speed, marginal cost toll or any combination thereof), and evaluate their impact on network performance when used as part of the distance-based tolling optimization framework. Investigating the impact of the number of tolling zones and the robustness of the tolling zone definitions to other types of non-recurrent events is also an interesting avenue for future research.

Author statement

The authors confirm contribution to the paper as follows:

CRediT authorship contribution statement

Antonis F. Lentzakis: Conceptualization, Methodology, Visualization, Investigation, Formal analysis, Writing - original draft, Writing - review & editing. **Ravi Seshadri:** Conceptualization, Methodology, Visualization, Investigation, Formal analysis, Writing - original draft, Writing - review & editing. **Arun Akkinepally:** Conceptualization, Methodology, Formal analysis, Writing - original draft, Writing - review & editing. **Vinh-An Vu:** Conceptualization, Methodology, Software, Validation, Data curation, Writing - review & editing. **Moshe Ben-Akiva:** Conceptualization, Methodology, Supervision, Writing - review & editing.

Acknowledgements

This research was supported by the National Research Foundation of Singapore through the Singapore-MIT Alliance for Research and Technology's FM IRG research programme.

Appendix A. Choice model parameters

The parameters of the pre-trip choice model are summarized in Table 6. The mean and standard deviation of the value of time are S$23.5 and S$5.75 respectively. Note that the cost coefficient is not shown in Table 6 since it is computed for each vehicle based on the sampled value of time (from the lognormal distribution).

Table 6
Pre-trip Behavioral Model - Parameters.

Parameter	Value
$ascCM$	−0.5
$ascCT$	−12
$ascCDT_1$	−0.12
$ascCDT_2$	−0.79
$ascCDT_3$	−1.15
$ascCDT_4$	−1.65
β_t^v	−0.008
β_{early}	−0.004
β_{late}	−0.016
VOT (Mean)	23.5
VOT (Std. Dev)	5.75

Appendix B. Supplementary results

The Kernel density functions for the differences in toll charged and travel time improvement for scenarios S1-S6 (Singapore network), relative to the base scenario are shown in Figs. 13 and 12 (corresponding to the ECDF shown in Fig. 9b, c and d). In addition, the distributions are summarized in Table 7.

Finally, the optimized tolling function parameters (Scenario S6) for selected time intervals of a single zone (arbitrarily selected) is provided in Table 8 below (note that the tolling function is of the form $a + bx$ where a is in S$, b is in S$ per kilometre and x is the distance traveled within the zone in kilometres).

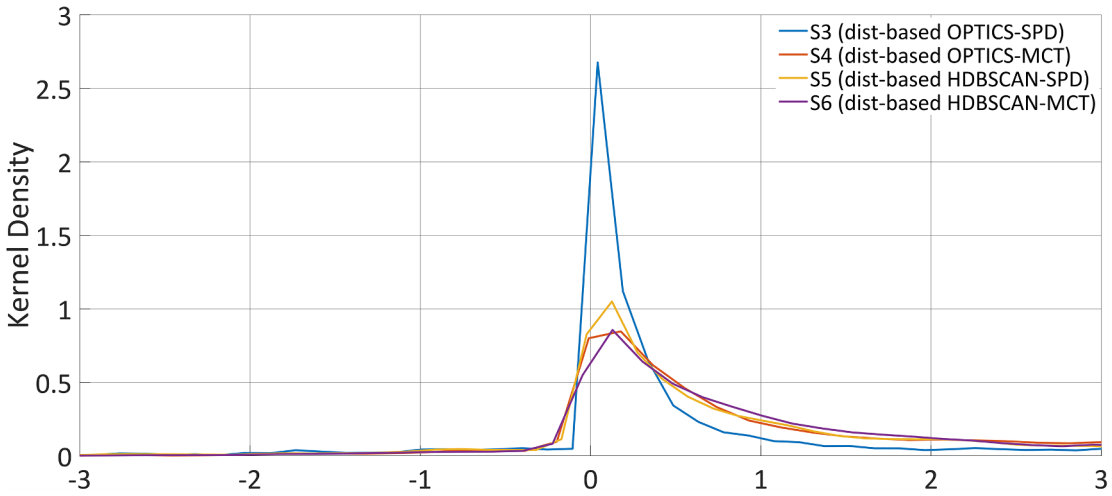

Fig. 12. Kernel density function of difference of total Toll Charge per OD-pair from **S0** for scenarios **S3**, **S4**, **S5**, **S6**.

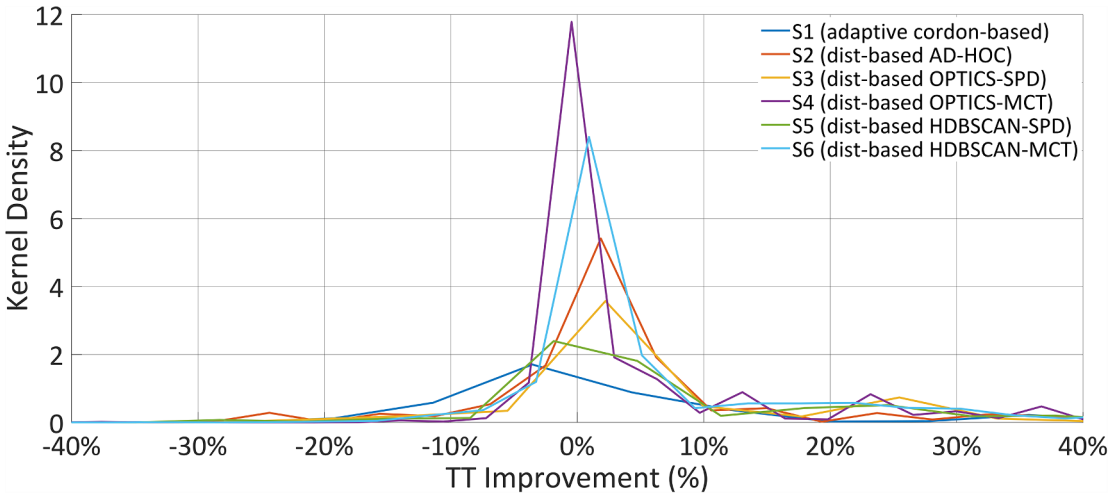

Fig. 13. Kernel density function for TT improvement per OD-pair over **S0** for scenarios **S1**, **S2**, **S3**, **S4**, **S5**, **S6**.

Table 7
Travel Time and Toll Charge Quartiles and Mean for **S1**, **S2**, **S3**, **S4**, **S5**, **S6**.

	Scenarios											
Toll($)/TT(s)	*S1*		*S2*		*S3*		*S4*		*S5*		*S6*	
Q1	0	249	0	248	0.01	247	0.12	237	0.07	243	0.11	240
Q2	0	457	0	456	0.16	452	0.47	437	0.36	453	0.46	440
Q3	0	705	0.39	689	0.56	694	1.45	665	1.12	695	1.42	671
Mean	0.27	586.3	0.49	564.6	0.58	577.8	1.0	511.2	0.82	559.4	0.98	512.5

Table 8
Example tolling function parameters for selected zone.

S.No	Tolling Function Parameters	
	a (S$)	b (S$/km)
1	0.18	0.87
2	0.40	0.95
3	2.51	0.96
4	1.79	0.04
5	0.33	0.13

Appendix C. Clustering with speed and marginal cost tolls

In this appendix, 2 additional models or scenarios are considered for the Singapore network, which involve dynamic predictive tolls computed using the framework described in Section 2. Scenarios **S7** and **S8** are variants of the predictive distance-based tolling scheme, whose tolling zone definitions were derived from a combination of speed and marginal cost toll data. Scenario **S7** (termed **OPTICS-SPD-MCT**) involves tolling zone definitions derived from the clusters obtained based on speed and marginal cost toll data using OPTICS. Scenario **S8** (termed **HDBSCAN*-SPD-MCT**), involves tolling zone definitions derived from speed and marginal cost toll data using HDBSCAN*. Similar to scenarios **S0**-**S6**, **S7** and **S8** are evaluated on the basis of the consumer surplus (CS) and average travel time (TT), in addition to the main performance measure, the total social welfare (SW). As is evident from the results of Table 9, the performance of falls between that of scenarios **S3**-**S4**, while that of **S8** falls between that of scenarios **S5**-**S6**. This is intuitive given

Table 9
Performance metrics SW, CS and TT for **S7**, **S8**.

	Scenarios	
Metrics	*S7*	*S8*
SW ($)	297592.5	328726.8
CS ($)	49345.0	104681.6
TT (s)	545.9	544.4

that all features are weighted equally, and confirms the original conclusion, that the best performance in terms of social welfare and network congestion comes from the use of tolling zone definitions derived from link marginal cost tolls (MCT), rather than speed data, or a combination of speed and marginal cost toll data.

Appendix D. Marginal cost tolls on selected links

Fig. 14 below shows the variation in the marginal cost tolls over time for selected links for the Singapore network. While there is definitely variation across time intervals, large fluctuations across successive time intervals is relatively rare, whereas systematic trends are certainly evident. For example, link 1119 (Fig. 14b) has two periods of significant congestion and overall, leads to a high MCT, whereas link 397 (Fig. 14c) has a larger period of relatively moderate congestion leading to an overall moderate MCT. In contrast, link 1063 (Fig. 14a) is rather uncongested throughout and overall has low MCT value. Our main considerations in using the average were twofold.

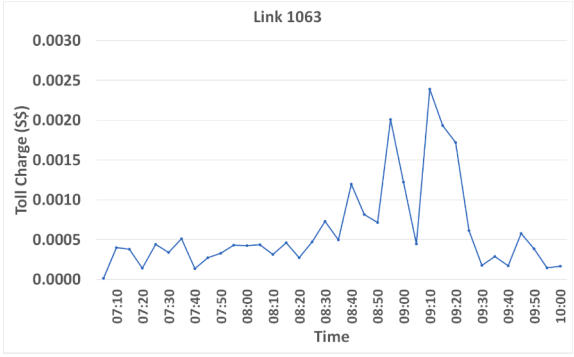

(a) Marginal cost tolls: Link 1063

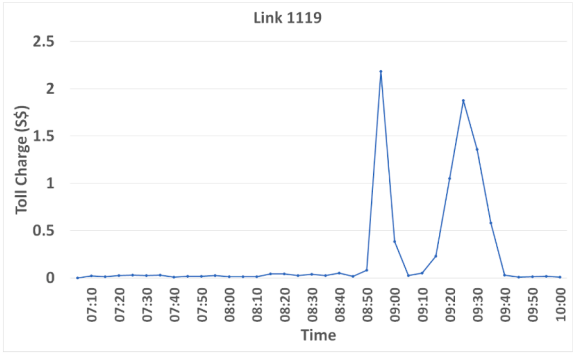

(b) Marginal cost tolls: Link 1119

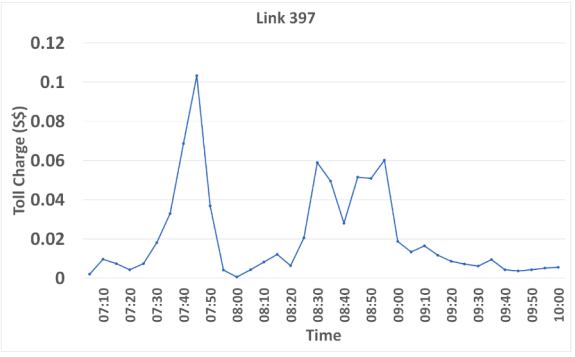

(c) Marginal cost tolls: Link 397

Fig. 14. Marginal cost tolls on selected links.

References

Ankerst, M., Breunig, M.M., Kriegel, H.P., Sander, J., 1999. Optics: ordering points to identify the clustering structure. In: ACM Sigmod Record. ACM, pp. 49–60.
Azevedo, C.L., Seshadri, R., Gao, S., Atasoy, B., Akkinepally, A.P., Christofa, E., Zhao, F., Trancik, J., Ben-Akiva, M., 2018. Tripod: sustainable travel incentives with prediction. In: The 97th Annual Meeting of Optimization, and Personalization. Transportation Research Board.
Ben-Akiva, M., Koutsopoulos, H.N., Antoniou, C., Balakrishna, R., 2010. Fundamentals of Traffic Simulation. New York, NY. chapter 10-Traffic Simulation with DynaMIT. International Series in Operations Research and Management Science.
Bonsall, P.W., Palmer, I.A., 1997. Do time-based road-user charges induce risk-taking? - results from a driving simulator. Traffic Eng. Control 38, 200–203.
Campello, R.J., Moulavi, D., Sander, J., 2013. Density-based clustering based on hierarchical density estimates. In: Pacific-Asia Conference on Knowledge Discovery and Data Mining. Springer, pp. 160–172.
Daganzo, C.F., Lehe, L.J., 2015. Distance-dependent congestion pricing for downtown zones. Transp. Res. Part B 75, 91–99.
Davies, D.L., Bouldin, D.W., 1979. A cluster separation measure. IEEE Trans. Pattern Anal. Mach. Intell. 1, 224–227.
Deb, K., Pratap, A., Agarwal, S., Meyarivan, T., 2002. A fast and elitist multiobjective genetic algorithm: Nsga-ii. IEEE Trans. Evolution. Comput. 6, 182–197.
Ferrari, P., 2002. Road network toll pricing and social welfare. Transp. Res. Part B 36, 471–483.
Florian, M.A., Morosan, C.D., 2014. A network model for capped distance-based tolls. CIRRELT.
Geroliminis, N., Levinson, D.M., 2009. Cordon pricing consistent with the physics of overcrowding. In: Transportation and Traffic Theory 2009. Springer, Golden Jubilee, pp. 219–240.

Gu, Z., Saberi, M., 2019a. A bi-partitioning approach to congestion pattern recognition in a congested monocentric city. Transp. Res. Part C: Emerg. Technol. 109, 305–320.
Gu, Z., Saberi, M., 2019b. A simulation-based optimization framework for urban congestion pricing considering travelers' departure time rescheduling. In: 2019 IEEE Intelligent Transportation Systems Conference (ITSC). IEEE, pp. 2557–2562.
Gu, Z., Shafiei, S., Liu, Z., Saberi, M., 2018. Optimal distance-and time-dependent area-based pricing with the network fundamental diagram. Transp. Res. Part C: Emerg. Technol. 95, 1–28.
Gupta, S., Seshadri, R., Atasoy, B., Pereira, F.C., Wang, S., Vu, V.A., Tan, G., Dong, W., Lu, Y., Antoniou, C., Ben-Akiva, M., 2016. Real time optimization of network control strategies in dynamit2. 0. In: Transportation Research Board 95th Annual Meeting.
Gupta, S., Seshadri, R., Atasoy, B., Prakash, A.A., Pereira, F., Tan, G., Ben-Akiva, M., 2020. Real-time predictive control strategy optimization. Transp. Res. Rec. https://doi.org/10.1177/0361198120907903.
Ji, Y., Geroliminis, N., 2012. On the spatial partitioning of urban transportation networks. Transp. Res. Part B: Methodol. 46, 1639–1656.
Ji, Y., Luo, J., Geroliminis, N., 2014. Empirical observations of congestion propagation and dynamic partitioning with probe data for large-scale systems. Transp. Res. Rec. J. Transp. Res. Board 2422, 1–11.
Kirk, R.S., Levinson, M., 2016. Mileage-Based Road User Charges. Technical Report. Congressional Research Service.
Lentzakis, A.F., Su, R., Wen, C., 2014. Time-dependent partitioning of urban traffic network into homogeneous regions. In: Control Automation Robotics & Vision (ICARCV), 2014 13th International Conference on. IEEE, pp. 535–540.
Li, M.Z., Lau, D.C., Seah, D.W., 2011. Car ownership and urban transport demand in singapore. Int. J. Transp. Econ./Rivista internazionale di economia dei trasporti 47–70.
Litman, T., 2014. Congestion Costing Critique Critical Evaluation of the Urban Mobility 2014 Report. Technical Report. Victoria Transport Policy Institute.
Liu, Z., Wang, S., Meng, Q., 2014. Optimal joint distance and time toll for cordon-based congestion pricing. Transp. Res. Part B 69, 81–97.
Lu, L., Xu, Y., Antoniou, C., Ben-Akiva, M., 2015a. An enhanced spsa algorithm for the calibration of dynamic traffic assignment models. Transp. Res. Part C: Emerg. Technol. 51, 149–166.
Lu, Y., Seshadri, R., Pereira, F., OSullivan, A., Antoniou, C., Ben-Akiva, M., 2015b. Dynamit2.0: Architecture design and preliminary results on real-time data fusion for traffic prediction and crisis management. In: Proceedings of IEEE 18th International Conference on Intelligent Transportation Systems, Spain. pp. 2250–2255.
McInnes, L., Healy, J., 2017. Accelerated hierarchical density based clustering. In: Data Mining Workshops (ICDMW), 2017 IEEE International Conference on. IEEE, pp. 33–42.
Meng, Q., Liu, Z., Wang, S., 2012. Optimal distance tolls under congestion pricing and continuously distributed value of time. Transp. Res. Part E: Logist. Transp. Rev. 48, 937–957.
de Palma, A., Lindsey, R., 2011. Traffic congestion pricing methodologies and technologies. Transp. Res. Part C: Emerg. Technol. 19, 1377–1399.
Rousseeuw, P.J., 1987. Silhouettes: a graphical aid to the interpretation and validation of cluster analysis. J. Comput. Appl. Math. 20, 53–65.
Saeedmanesh, M., Geroliminis, N., 2017. Dynamic clustering and propagation of congestion in heterogeneously congested urban traffic networks. Transp. Res. Procedia 23, 962–979.
Schubert, E., Sander, J., Ester, M., Kriegel, H.P., Xu, X., 2017. Dbscan revisited, revisited: why and how you should (still) use dbscan. ACM Trans. Database Syst. (TODS) 42, 19.
Simoni, M., Pel, A., Waraich, R., Hoogendoorn, S., 2015. Marginal cost congestion pricing based on the network fundamental diagram. Transp. Res. Part C: Emerg. Technol. 56, 221–238.
Simoni, M.D., Kockelman, K.M., Gurumurthy, K.M., Bischoff, J., 2019. Congestion pricing in a world of self-driving vehicles: An analysis of different strategies in alternative future scenarios. Transp. Res. Part C: Emerg. Technol. 98, 167–185.
Small, K.A., Verhoef, E.T., 2007. The Economics of Urban Transportation. Routledge.
Smith, M.J., May, A.D., Wisten, M.B., Milne, D.S., Van Vliet, D., Ghali, M.O., 1994. A comparison of the network effects of four road-user charging systems. Traffic Eng. Control 35, 311–315.
Sun, X., Liu, Z., Thompson, R., Bie, Y., Weng, J., Chen, S., 2016. A multi-objective model for cordon-based congestion pricing schemes with nonlinear distance tolls. J. Central South Univ. 23, 1273–1282.
Yang, H., Huang, H.J., 1998. Principle of marginal-cost pricing: how does it work in a general road network? Transp. Res. Part A: Policy Pract. 32, 45–54.
Yang, L., Saigal, R., Zhou, H., 2012. Distance-based dynamic pricing strategy for managed toll lanes. Transp. Res. Rec. J. Transp. Res. Board 2283, 90–99.
Zheng, N., Rérat, G., Geroliminis, N., 2016. Time-dependent area-based pricing for multimodal systems with heterogeneous users in an agent-based environment. Transp. Res. Part C: Emerg. Technol. 62, 133–148.
Zheng, N., Waraich, R.A., Axhausen, K.W., Geroliminis, N., 2012. A dynamic cordon pricing scheme combining the macroscopic fundamental diagram and an agent-based traffic model. Transp. Res. Part A: Policy Pract. 46, 1291–1303.
Zhu, F., Ukkusuri, S.V., 2015. A reinforcement learning approach for distance based dynamic tolling in the stochastic network environment. J. Adv. Transp. 49, 247–266.